European Polymer Journal 46 (2010) 1355–1366

Contents lists available at ScienceDirect

European Polymer Journal

journal homepage: www.elsevier.com/locate/europolj

Synthesis and characterization of electrochromic poly(amide–imide)s based on the diimide-diacid from 4,4′-diamino-4″-methoxytriphenylamine and trimellitic anhydride

Sheng-Huei Hsiao [a,*], Guey-Sheng Liou [b], Yi-Chun Kung [c], Yi-Ju Lee [c]

[a] Department of Chemical Engineering and Biotechnology, National Taipei University of Technology, Taipei 10608, Taiwan
[b] Institute of Polymer Science and Engineering, National Taiwan University, Taipei 10617, Taiwan
[c] Department of Chemical Engineering, Tatung University, Taipei 10451, Taiwan

ARTICLE INFO

Article history:
Received 18 February 2010
Received in revised form 19 March 2010
Accepted 23 March 2010
Available online 27 March 2010

Keywords:
Poly(amide–imide)s
Triphenylamine
Electrochemistry
Cyclic voltammetry
Electrochromism

ABSTRACT

A dicarboxylic acid bearing two preformed imide rings, namely 4,4′-bis(trimellitimido)-4″-methoxytriphenylamine (**3**), was prepared by the condensation of 4,4′-diamino-4″-methoxytriphenylamine (**2**) and two molar equivalents of trimellitic anhydride (TMA). A new family of aromatic poly(amide–imide)s (PAIs) containing the electroactive triphenylamine (TPA) unit were prepared by the triphenyl phosphite activated polycondensation of the diimide-diacid **3** with various aromatic diamines. All the polymers were readily soluble in many organic solvents and could be solution-cast into tough and flexible polymer films. They displayed high glass-transition temperatures (269–313 °C) and good thermal stability, with 10% weight-loss temperatures in excess of 521 °C in nitrogen and char yields at 800 °C in nitrogen higher than 68%. Cyclic voltammograms of the PAI films cast onto an indium–tin oxide (ITO)-coated glass substrate exhibited one reversible oxidation redox couple at 0.91–0.93 V vs. Ag/AgCl in acetonitrile solution. The polymer films revealed a good electrochemical and electrochromic stability, with a color change from colorless neutral form to blue oxidized form at applied potentials ranging from 0.0 to 1.2 V. The PAIs containing the TPA unit in both imide and amide segments showed multicolor electrochromism: pale yellow in the neutral state, green in the semi-oxidized state, and deep blue in the fully oxidized state.

1. Introduction

The ability of reversible change in the transmitted or reflected light upon electrochemical oxidation or reduction of electrochromic materials has aroused the interest of scientists over the past decades [1]. Electrochromic properties have proved promising for automatic anti-glazing mirror, smart windows, electrochromic displays, and chameleon materials [2–10]. There are many chemical systems that are intrinsically electrochromic, such as transition metal oxides, inorganic coordination complexes, organic molecules, and conjugated polymers [11–15]. Among the available electrochromic materials, conjugated polymers represented by polypyrrole and poly(3,4-ethylenedioxythiophene) (PEDOT) and their derivatives have received a great deal of attention because of their attractive electrochromic properties, such as fast response time, high coloration efficiency and contrast ratio, good stability, and wide range of colors [16–25].

Triphenylamine (TPA)-based starbursts, dendrimers, and polymers are not only promising photoconductors and hole transport materials for electro-optical applications [26,27], but also show interesting electrochromic behavior [28,29]. In recent years, the Liou's and our groups have carried out extensive studies on the design and synthesis of TPA-based high-performance polymers such as

* Corresponding author. Tel.: +886 2 27712171x2548; fax: +886 2 27317117.
E-mail address: shhsiao@ntut.edu.tw (S.-H. Hsiao).

0014-3057/$ - see front matter © 2010 Elsevier Ltd. All rights reserved.
doi:10.1016/j.eurpolymj.2010.03.016

aromatic polyamides and polyimides for potential electrochromic applications [30–36]. Two basic properties of the TPA unit are the easy oxidizability of the amino center and its ability to transport positive charge centers via the radical cation species.

Aromatic polyimides possess desirable characteristics such as high thermal stability and excellent physical properties [37]. However, their applications have been limited owing to their poor solubility and intractable characteristics. Replacement of polyimides by copolyimides such as poly(amide–imide)s (PAIs) may be useful in modifying the intractable character of polyimides [38–40]. Because of containing both amide and imide groups in polymer repeating units, PAIs have properties between polyamides and polyimides; accordingly, this class of polymers offers a good compromise between high thermal property and processability. Since we successfully applied the Yamazaki–Higashi phosphorylation reaction [41] to the direct synthesis of high-molecular-weight PAIs from the TMA-derived imide ring-bearing dicarboxylic acids and aromatic diamines using triphenyl phosphite (TPP) and pyridine as condensing agents [42,43], this efficient synthetic route has proved to exhibit significant advantages in preparing operations as compared with conventional acid chloride or isocyanate methods. Thus, many novel PAIs have been readily prepared by this convenient technique in our and other laboratories [44–48]. Furthermore, this synthetic procedure can offer us the option of the incorporation of specific functionalities between amide or imide groups in the PAI backbone. The incorporation of such functional groups may provide a method of controlling certain physical properties or special functions of the resulting PAIs. As a continuation of our efforts in developing easily processable high-performance functional polymers with the TPA moieties, the present study describes the synthesis of novel electrochromic PAIs based on a new diimide-dicarboxylic acid **3** condensed from 4,4′-diamino-4″-methoxytriphenylamine (**2**) and TMA. The active sites of the TPA unit are blocked with electron-donating methoxy substituent; thus, the present PAIs are expected to exhibit an increased electrochemical and electrochromic stability.

2. Experimental

2.1. Materials

According to the reported procedures, the TPA-based diamine monomers that included 4,4′-diaminotriphenylamine (mp = 186–187 °C) [49], 4,4′-diamino-4″-methoxytriphenylamine (**2**) (mp = 150–152 °C) [32], and 4,4′-diamino-4″-*tert*-butyltriphenylamine (**4f**) (mp = 113–115 °C) [31], were synthesized by the cesium fluoride (CsF)-mediated aromatic nucleophilic substitution reaction of *p*-fluoronitrobenzene with aniline, *p*-anisidine (4-methoxyaniline), and 4-*tert*-butylaniline, respectively, followed by Pd/C-catalyzed hydrazine reduction of the intermediate dinitro compounds. *p*-Fluoronitrobenzene (Acros), 10% palladium on charcoal (Pd/C) (Fluka), CsF (Acros), *p*-anisidine (Acros), triphenyl phosphite (TPP) (Acros), hydrazine monohydrate (TCI), *N,N*-dimethylformamide (DMF) (Acros), and dimethyl sulfoxide (DMSO) (Tedia) were used without further purification. *N,N*-Dimethylacetamide (DMAc) (Tedia), *N*-methyl-2-pyrrolidinone (NMP) (Tedia), and pyridine (Py) (Wako) were dried over calcium hydride for 24 h, distilled under reduced pressure, and stored over 4 Å molecular sieves in a sealed bottle. Trimellitic anhydride (TMA) (Wako) was dried at 250 °C *in vacuo* for 3 h before use. The commercially available diamines such *p*-phenylenediamine (**4a**) (TCI), *m*-phenylenediamine (**4b**) (Acros), 4,4′-oxydianiline (**4c**) (TCI), 3,4′-oxydianiline (**4d**) (TCI), 9,9-bis(4-aminophenyl)fluorene (**4e**) (TCI), were used as received. All other reagents were used as received from commercial sources.

2.2. Synthesis of 4,4′-bis(trimellitimido)-4″-methoxytriphenylamine (*3*)

A flask was charged with 3.05 g (0.01 mol) of 4,4′-diamino-4″-methoxytriphenylamine (**2**), 3.84 g (0.02 mol) of trimellitic anhydride, and 60 mL of glacial acetic acid. The heterogeneous mixture was stirred for 1 h and then refluxed at 140 °C for 12 h. The reaction mixture was cooled to precipitate a yellowish brown powder which was rinsed with methanol to remove acetic acid. The obtained crude product was washed several times with hot water and then recrystallized from acetic acid. The product was filtered to afford 5.23 g (80% in yield) orange crystal. Mp: 294–298 °C measured by DSC at 10 °C/min. IR (KBr): 3700–2400 cm^{-1} (OH stretch); 1778, 1716 cm^{-1} (imide C=O); 1695 cm^{-1} (acid C=O). ^1H NMR (500 MHz, DMSO-d_6, δ, ppm): 3.78 (s, 3H, OCH_3), 7.02 (d, J = 9.0 Hz, 2H, H_a), 7.12 (d, J = 8.9 Hz, 4H, H_c), 7.19 (d, J = 8.9 Hz, 2H, H_b), 7.36 (d, J = 8.9 Hz, 4H, H_d), 8.07 (d, J = 7.8 Hz, 2H, H_g), 8.29 (s, 2H, H_e), 8.41 (d, J = 7.8 Hz, 2H, H_f). ^{13}C NMR (125 MHz, DMSO-d_6, δ, ppm): 55.2 (OCH_3), 115.3 (C^2), 121.9 (C^6), 123.2 (C^{11}), 123.6 (C^{14}), 125.3 (C^{10}), 128.2 (C^3, C^7), 131.9 (C^{15}), 134.8 (C^{12}), 135.3 (C^{13}), 136.4 (C^5), 139.0 (C^4), 1463.9 (C^8), 156.7 (C^1), 165.7 (COOH), 166.3 (C^9), 166.3 (C^{16}).

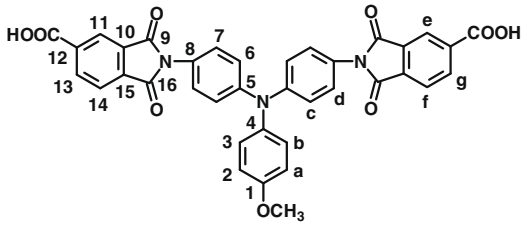

2.3. Synthesis of 4,4′-bis(trimellitimido)triphenylamine (*3′*)

According to the similar procedure as described above, diimide-diacid **3′** was synthesized from the condensation of 4,4′-diaminotriphenylamine and two molar equivalents of TMA with a 90% yield and mp of 288–291 °C (by DSC, 10 °C/min). IR (KBr): 3700–2400 cm^{-1} (OH stretch); 1778, 1716 cm^{-1} (imide C=O); 1699 cm^{-1} (acid C=O). ^1H NMR (500 MHz, DMSO-d_6, δ, ppm): 7.17 (m, 7H, H_{a+c+d}), 7.41 (m, 6H, H_{b+e}), 8.08 (d, J = 7.8 Hz, 2H, H_f), 8.31 (s, 2H, H_h), 8.41 (d, J = 8.0 Hz, 2H, H_g). ^{13}C NMR (125 MHz, DMSO-d_6, δ, ppm): 123.3 (C^6), 123.3 (C^3), 123.7 (C^{11}), 124.2 (C^1), 125.1 (C^{14}), 126.2 (C^2), 128.4 (C^7), 129.9 (C^{13}), 132.0 (C^8),

134.9 (C^5), 135.4 (C^4), 136.6 (C^{12}), 146.6 (C^{10}), 146.79 (C^{15}), 165.8 (COOH), 166.4 (C^{16}, C^9).

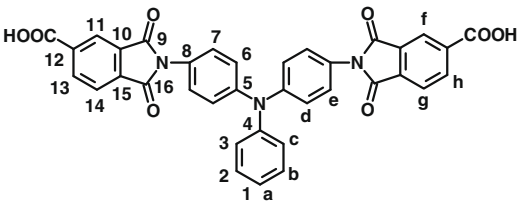

2.4. Synthesis of PAIs

The synthesis of PAI **5a** was used as an example to illustrate the general synthetic route used to produce the PAIs. A mixture of 0.654 g (1.0 mmol) of the diimide-diacid monomer **3**, 0.108 g (1.0 mmol) of *p*-phenylenediamine (**4a**), 0.15 g of anhydrous calcium chloride, 1.2 mL of triphenyl phosphite (TPP), 0.4 mL of pyridine, and 1.5 mL of NMP was heated with stirring at 120 °C for 3 h. The resulting polymer solution was poured slowly into 200 mL of stirred methanol giving rise to a tough, fiber-like precipitate that was collected by filtration, washed thoroughly with hot water and methanol, and dried.

2.5. Preparation of the PAI films

A solution of the polymer was made by dissolving about 0.6 g of the PAI sample in 8 mL of hot DMAc. The homogeneous solution was poured into a 7-cm glass Petri dish, which was placed in a 90 °C oven overnight for the slow release of the solvent, and then the film was stripped off from the glass substrate and further dried in vacuum at 160 °C for 6 h. The obtained films were about 0.09 mm thick and were used for X-ray diffraction measurements, tensile test, solubility tests, and thermal analyses.

2.6. Measurements

Infrared (IR) spectra were recorded on a Horiba FT-720 FT-IR spectrometer. ^{1}H and ^{13}C NMR spectra were measured on a Bruker AVANCE 500 FT-NMR system with tetramethylsilane as an internal standard. The inherent viscosities were determined with a Cannon–Fenske viscometer at 30 °C. Wide-angle X-ray diffraction (WAXD) measurements were performed at room temperature (ca. 25 °C) on a Shimadzu XRD-6000 X-ray diffractometer with a graphite monochromator (operating at 40 kV and 30 mA), using nickel-filtered Cu-Kα radiation (λ = 1.5418 Å). The scanning rate was 2°/min over a range of 2θ = 10–40°. Thermogravimetric analysis (TGA) was performed with a Perkin-Elmer Pyris 1 TGA. Experiments were carried out on approximately 4–6 mg of samples heated in flowing nitrogen or air (flow rate = 40 cm^3/min) at a heating rate of 20 °C/min. DSC analyses were performed on a Perkin-Elmer Pyris 1 DSC at a scan rate of 20 °C/min in flowing nitrogen. Thermomechanical analysis (TMA) was determined with a Perkin-Elmer TMA 7 instrument. The TMA experiments were carried out from 50 to 350 °C at a scan rate of 10 °C/min with a penetration probe 1.0 mm in diameter under an applied constant load of 10 mN. Softening temperatures (T_s) were taken as the onset temperatures of probe displacement on the TMA traces. Ultraviolet–visible (UV–vis) spectra of the polymer films were recorded on an Agilent 8453 UV–visible spectrometer. Electrochemistry was performed with a CHI 611C electrochemical analyzer. Voltammograms are presented with the positive potential pointing to the left and with increasing anodic currents pointing downwards. Cyclic voltammetry was conducted with the use of a three-electrode cell in which ITO (polymer films area about 0.9 × 1.1 cm) was used as a working electrode. A platinum wire was used as an auxiliary electrode. All cell potentials were taken with the use of a home-made Ag/AgCl, KCl (sat.) reference electrode. Ferrocene was used as an external reference for calibration (+0.44 V vs. Ag/AgCl). Spectroelectrochemistry analyses were carried out with an electrolytic cell, which was composed of a 1 cm cuvette, ITO as a working electrode, a platinum wire as an auxiliary electrode, and a home-made Ag/AgCl, KCl (sat.) reference electrode. Absorption spectra in the spectroelectrochemical experiments were measured with an Agilent 8453 UV–visible photodiode array spectrophotometer. Coloration efficiency is derived from the equation: $\eta = \Delta OD/Q$, ΔOD is optical density change at specific absorption wavelength and Q is ejected charge determined from the in situ experiments. Photoluminescence (PL) spectra were measured with a Varian Cary Eclipse fluorescence spectrophotometer. Fluorescence quantum yields (Φ_F) values of the samples in NMP were measured by using quinine sulfate in 1 N H_2SO_4 as a reference standard (Φ_F = 0.546) [50]. All corrected fluorescence excitation spectra were found to be equivalent to their respective absorption spectra.

3. Results and discussion

3.1. Monomer synthesis

The new diimide-diacid monomer **3** containing the methoxyTPA unit was synthesized by the synthetic route outlined in Scheme 1. The methoxyTPA diamine **2** was prepared from the CsF-assisted *N,N*-diarylation of *p*-anisidine with *p*-fluoronitrobenzene, followed by hydrazine Pd/C-catalyzed reduction of the intermediate dinitro compound **1**. Synthetic details and characterization data of compounds **1** and **2** have been described in one of our previous publications [32]. The targeted diimide-diacid **3** was prepared by the condensation of **2** with two molar equivalents of TMA in refluxing glacial acetic acid. Fig. 1 illustrates the ^{1}H NMR and ^{13}C NMR spectra of **3**. Assignments of each carbon and hydrogen are assisted by the two-dimensional NMR spectrum shown in Fig. 2, and these spectra are in good agreement with the proposed molecular structure of **3**. The diimide-diacid **3′** (see Section 2) used for the synthesis of referenced PAIs **5′a–5′g** was also prepared following a similar procedure from 4,4′-diaminotriphenylamine and TMA.

3.2. Polymer synthesis

According to the phosphorylation polyamidation technique first described by Yamazaki and co-workers [41], a series of novel PAIs **5a–g** were synthesized from the

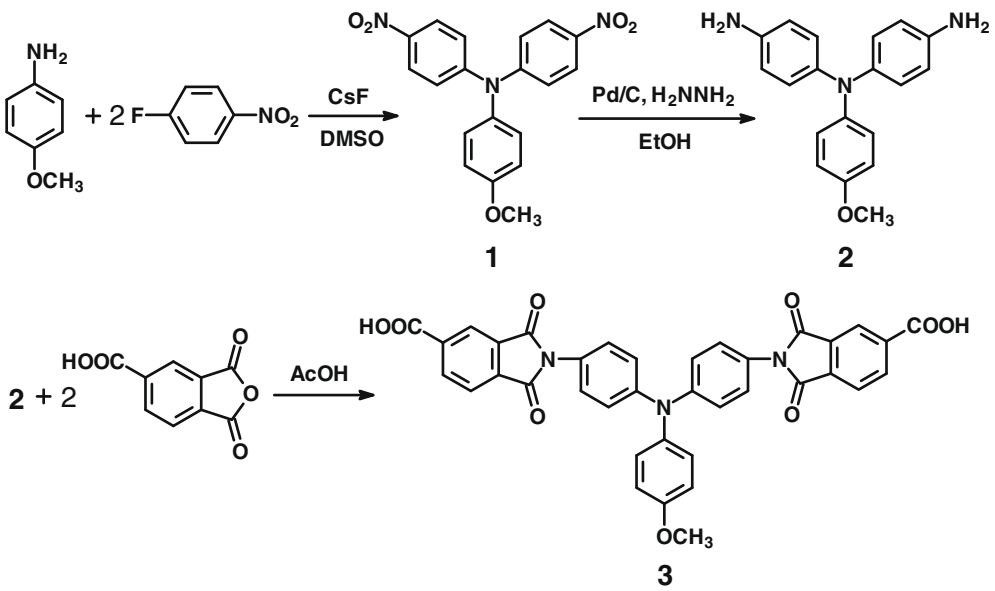

Scheme 1. Synthetic route to the diimide-diacid monomer **3**.

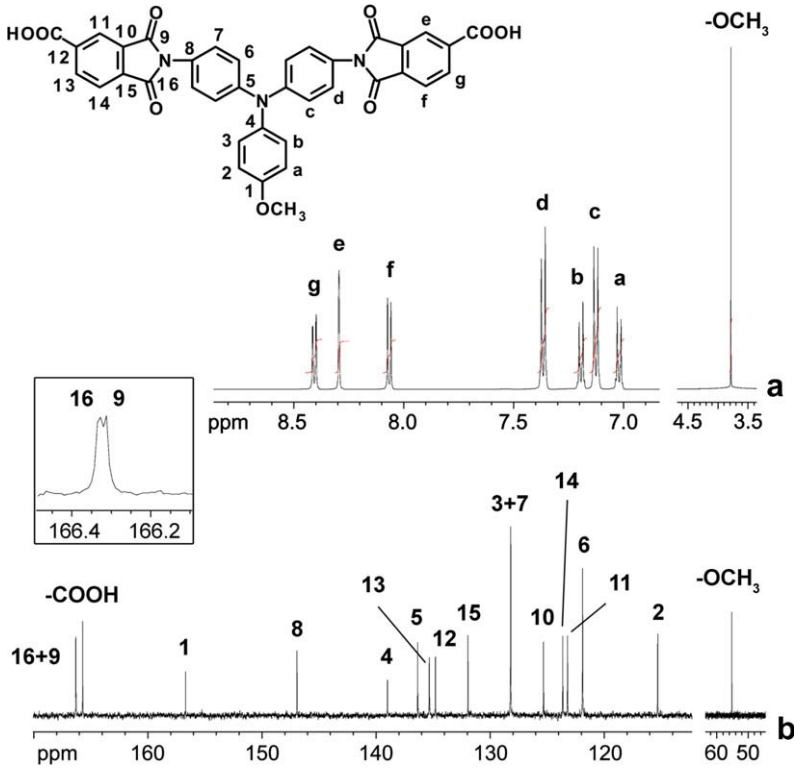

Fig. 1. (a) ^{1}H NMR and (b) ^{13}C NMR spectra of diimide-diacid **3** in DMSO-d_6.

polycondensation reactions of diimide-dicarboxylic acid **3** with various aromatic diamines **4a–4f** and **2** by using triphenyl phosphite (TPP) and pyridine as condensing agents (Scheme 2). The polymerization proceeded homogeneously throughout the reaction and afforded clear, highly viscous polymer solution. Except for **5a** all the polymers precipitated in a tough, fiber-like form when the resulting polymer solutions were slowly poured under stirring into methanol. These PAIs were obtained in almost quantitative yields, with inherent viscosity in the range of 0.33–0.65 dL/g, as

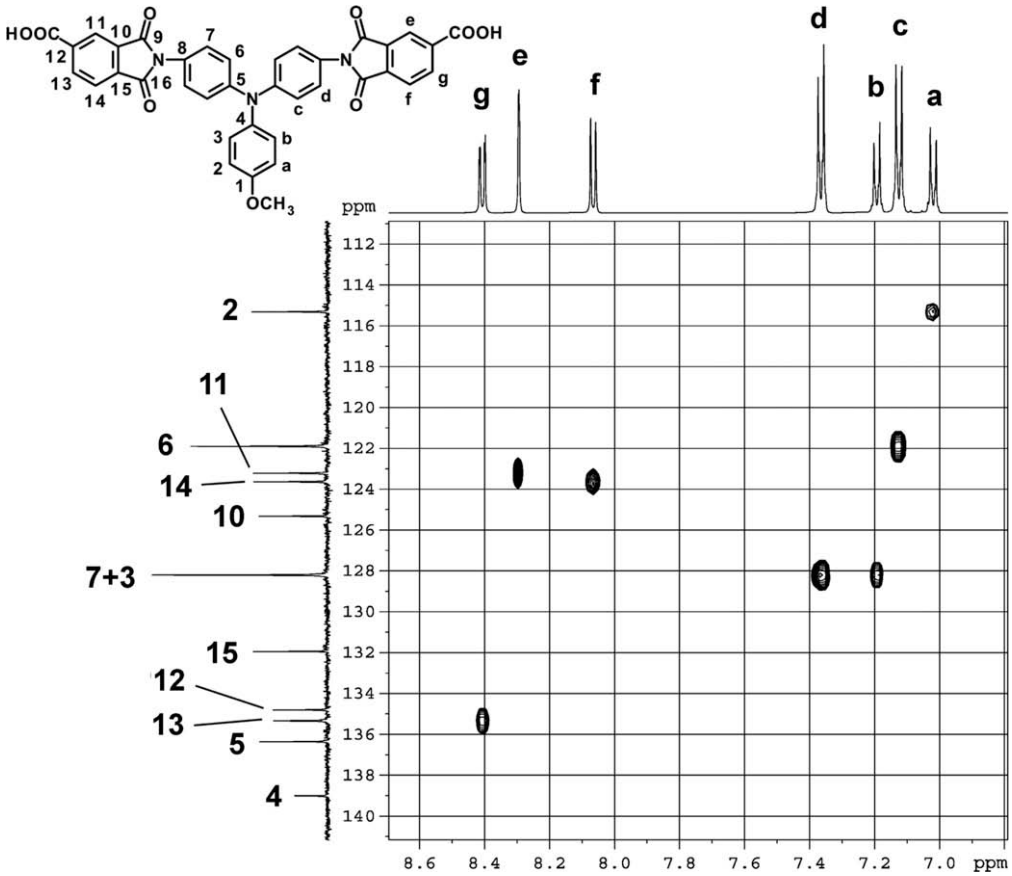

Fig. 2. C–H HMQC spectra of diimide-diacid **3** in DMSO-d_6.

summarized in Table 1. In the synthesis of **5a**, an early precipitation occurred due to insolubility of the polymer which led to an ineffective polymerization reaction. With the exception of **5a**, the polymers can be solution-cast into flexible and tough films, and this is indicative of the formation of high-molecular-weight polymers. Fig. 3 shows a typical IR spectrum for PAI **5c**, where we can assign the characteristic amide absorption bands at 3290 (N–H) and 1672 cm^{-1} (amide C=O), and the characteristic imide absorption bands at 1778 (asymmetrical C=O), 1720 (symmetrical C=O), 1385 (imide C–N), and 725 cm^{-1} (imide ring deformation). Fig. 4 shows a typical ^1H NMR spectrum of **5c** in deuterated dimethyl sulfoxide (DMSO-d_6). Assignments of each proton are assisted by the two-dimensional H–H COSY NMR spectrum, and the spectra agree well with the proposed molecular structure of **5c**.

3.3. Properties of PAIs

3.3.1. Organo-solubility and film morphology

The qualitative solubility of the synthesized PAIs is summarized in Table 1. Most of the PAIs were well dissolved in aprotic solvents such as NMP, DMAc, DMF, and DMSO at room temperature, and formed tough and transparent films by solution-casting. The good solubility of these PAIs could be attributed to the introduction of the three-dimensional TPA moiety and flexible pendent methoxy substituent (for the **5** series PAIs) into the repeat unit. In all cases, the **5** series PAIs showed a slightly enhanced solubility compared the corresponding **5′** ones. This may be a result of increased free volume and decreased interchain interactions caused by the methoxy substitution. Therefore, the good solubility makes these polymers potential candidates for practical applications in spin- or dip-coating and ink jet-printing processes. The PAIs **5a** and **5′a** derived from the more rigid *p*-phenylenediamine showed a decreased solubility and could not afford flexible films. The PAIs that could afford flexible and tough films were amorphous in nature as evidenced by wide-angle X-ray diffraction patterns.

3.3.2. Thermal properties

Thermal properties of the PAIs were investigated by DSC, TMA, and TGA. The results are summarized in Table 2. The glass-transition temperatures (T_gs) of the **5** series PAIs were observed in the range of 269–313 °C by DSC. The T_g order corresponds to the decreasing order of chain stiffness. The relatively lower T_g value of PAI **5d** can be explained in terms of the flexibility, low rotation barrier, and asymmetric *meta*-linkage of its diamine moiety. The highest T_g value associated with PAI **5e** can be attributed to the presence of rigid 9,9-diphenylfluorene unit in the

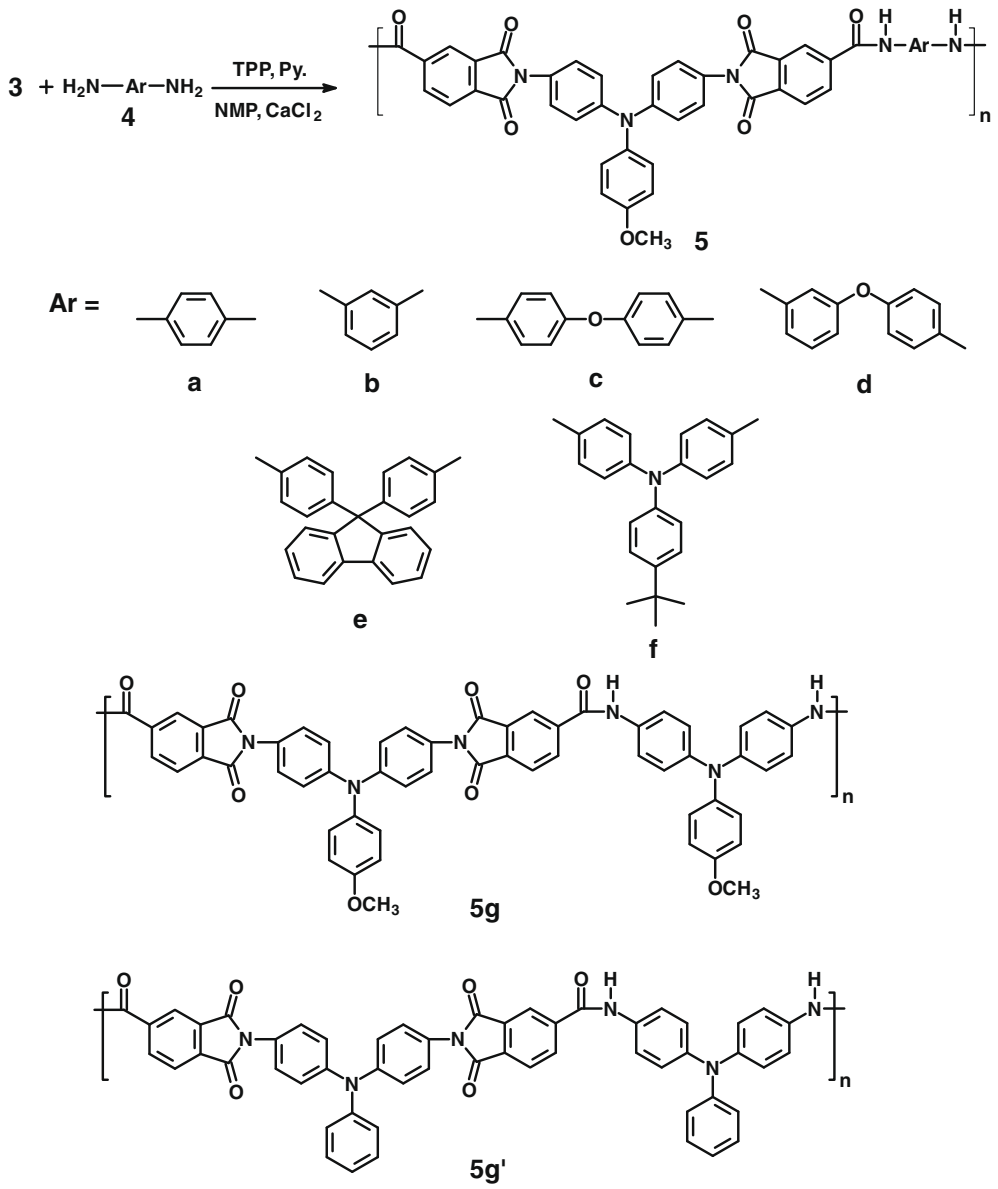

Scheme 2. Synthesis of PAIs **5a**–**5g**.

diamine component that stiffens the polymer backbone. For the polymers derived from the same diamine component, the **5** series PAIs showed lower T_g values as compared to the corresponding **5′** analogs. This may be rationalized by the increased free volume and decreased interchain interactions introduced by the methoxy substitution.

The softening temperatures (T_s) of the polymer films were determined with TMA by the penetration method. The T_s value was read from the onset temperature of the probe displacement on the TMA curve. Typical TMA curve for a representative PAI **5c** is illustrated in Fig. 5. The T_s values of the **5** series are in the range from 259 to 300 °C and the **5′** series PAIs are in the range from 255 to 305 °C. In most cases, the T_s values obtained by TMA are comparable to the T_g values measured by the DSC experiments.

The thermal stability of PAIs was evaluated by TGA in both air and nitrogen atmospheres. Typical TGA curves for PAIs **5c** are depicted in the inset of Fig. 5. The decomposition temperatures (T_d) at 10% weight losses in nitrogen and air atmosphere taken from the original TGA thermograms are given in Table 2. All of the polymers exhibited good thermal stability; the T_d of PAIs **5a**–**5g** at a 10% weight-loss were recorded in the range of 504–578 °C in nitrogen and 473–558 °C in air, respectively. The amount of carbonized residues (char yield) at 800 °C in nitrogen for all PAIs was in the range of 66–72 wt.%. The high char yields of these polymers can be attributed to their high aromatic content. It also can be seen from Table 2, the **5** series PAIs decomposed at a lower temperature than the corresponding **5′** PAIs because of the presence of less stable methoxy groups.

Table 1
Inherent viscosities and solubility behavior of poly(amide–imide)s.

Polymer code	η_{inh}[a] (dL/g)	Solubility in various solvents[b]					
		NMP	DMAc	DMF	DMSO	*m*-Cresol	THF
5a	0.33	++	+	+	+	++	±
5b	0.64	++	++	++	++	+	–
5c	0.65	++	++	++	++	+	–
5d	0.42	++	++	++	++	++	–
5e	0.41	++	++	++	++	++	–
5f	0.54	++	++	++	+	+	±
5 g	0.62	++	++	++	+	+	±
5′a	0.30	±	±	±	±	+	±
5′b	1.05	++	++	++	+	+	–
5′c	1.07	++	++	++	+	+	–
5′d	0.52	++	++	++	++	+	±
5′e	0.43	++	++	++	++	+	±
5′f	0.56	++	++	++	+	+	±
5′g	0.85	++	++	+	±	+	–

[a] Inherent viscosity measured at a concentration of 0.5 g/dL in DMAc-5 wt.% LiCl at 30 °C.
[b] The qualitative solubility was tested with 10 mg of a sample in 1 mL of stirred solvent. ++, soluble at room temperature; +, soluble on heating; ±, partially soluble on heating; –, insoluble even on heating. Solvent: NMP: *N*-methyl-2-pyrrolidone; DMAc: *N*,*N*-dimethylacetamide; DMF: *N*,*N*-dimethylformamide; DMSO: dimethyl sulfoxide; THF: tetrahydrofuran.

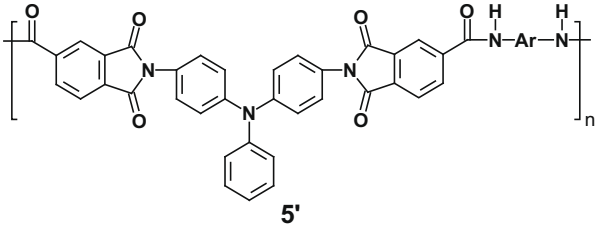

5'

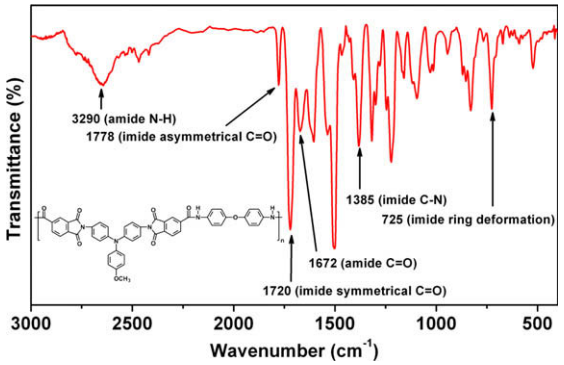

Fig. 3. IR spectrum (film) of PAI **5c**.

3.3.3. Optical and electrochemical properties

The optical properties of the PAIs are investigated by UV–vis and photoluminescence (PL) spectroscopy. The relevant data are summarized in Table 3. These polymers exhibit strong UV–vis absorption bands at 290–310 nm in NMP solution, which are peculiar to the combinations of n–π^* and π–π^* transitions resulting from the conjugated methoxyTPA segment. In solid state, the UV–vis absorptions of PAIs are nearly identical and show absorbance maxima around 311–318 nm. These methoxyTPA-based PAIs exhibited fluorescence emission maxima around 363–366 nm in NMP solution. All the PAIs generally showed very low quantum yields due to the effectively charge-transfer complex formation caused by the extremely electron-donating methoxyTPA moiety to the electron-accepting trimellitimide unit.

The electrochemical behavior of PAIs was investigated by cyclic voltammetry (CV) conducted for the cast film on an ITO-coated glass slide as working electrode in dry acetonitrile (CH_3CN) containing 0.1 M of tetrabutylammonium perchlorate (TBAP) as an electrolyte under nitrogen atmosphere. The representative cyclic voltammogram for PAI **5c** is shown in Fig. 6. There is one reversible oxidation redox couples at half-wave potentials ($E_{1/2}$) of 0.91 V in the oxidative scan. PAI **5c** exhibited good electrochemical redox stability by repetitive cycling between 0.0 and 1.05 V (at least 50 cycles). We also noted the color of the film changed from yellow to blue as the electrode potential was raised to 1.05 V. Comparing the electrochemical data, it was found that PAI **5c** is more easily oxidized than PAI **5′c** without the methoxy substituents ($E_{1/2}$ values: 0.91 vs. 1.06 V). Obviously, the lower oxidative potential for PAI **5c** compared to **5′c** can be attributed to the electron-donating methoxy substituent. There are two well-defined and reversible oxidation redox couples for the PAIs (**5f** and **5g**) containing the TPA unit in both the amide and imide segments. For example, the $E_{1/2}$ values of the PAI **5g** were observed at 0.74 and 0.93 V, respectively (Fig. 7). The first electron removal for PAI **5g** was assumed to occur at the amino center in the amide segment, which should be more electron-richer than the amino center in the imide segment. As expected, PAI **5′g** showed a delayed oxidation, with $E_{1/2}$ = 0.86 and 1.04 V, in comparison to **5g** because of no methoxy substitution on TPA. During the CV scanning,

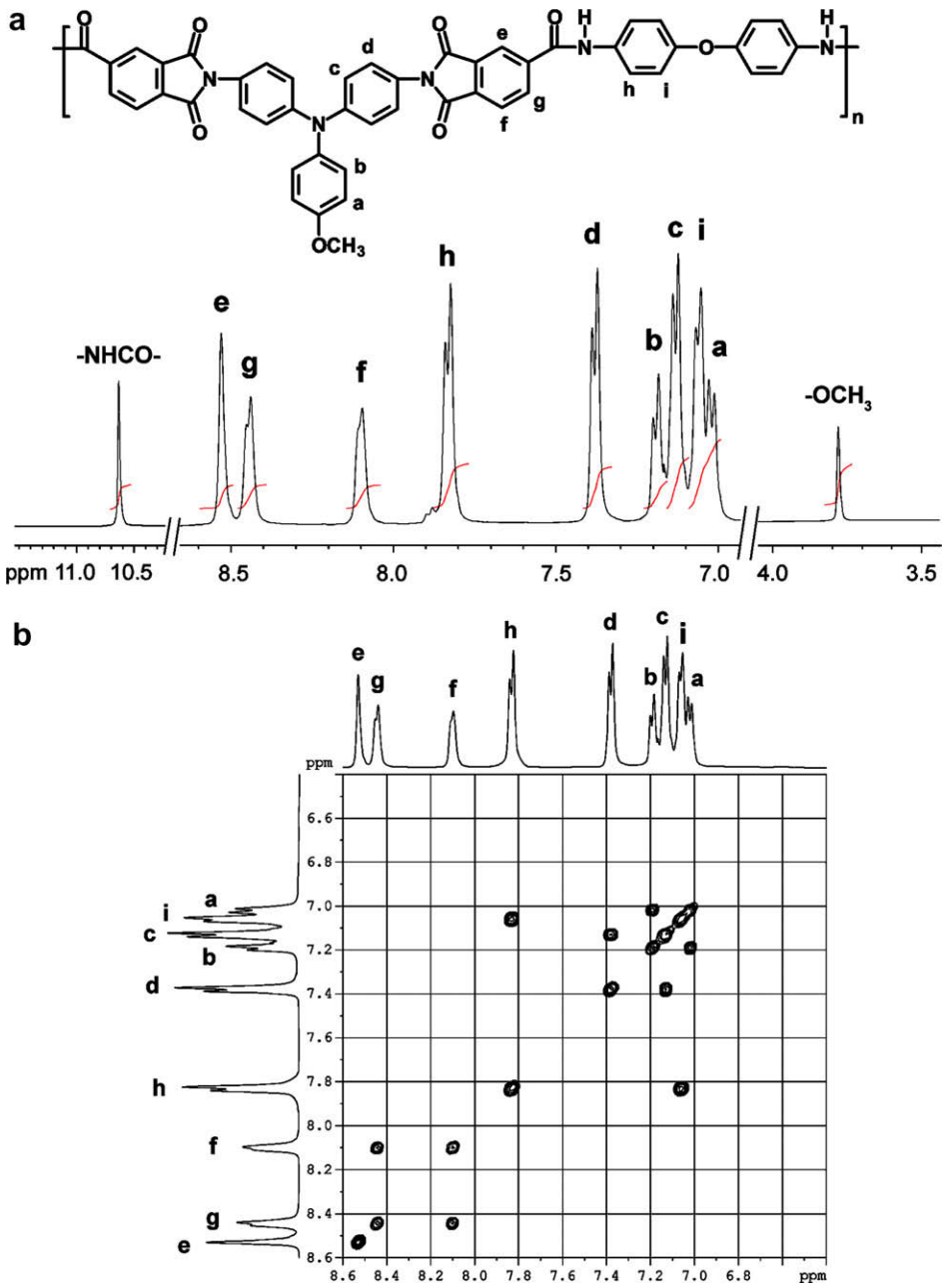

Fig. 4. (a) ^{1}H NMR and (b) H–H COSY spectra of PAI **5c** in DMSO-d_6.

we also found these PAIs showed interesting multi-electrochromic behaviors. For example, the color of **5f** and **5g** films changed from pale yellow to green, then to deep blue, corresponding to two electrochemical oxidation processes of the polymers. The energy levels of the HOMO and LUMO of the investigated PAIs can be estimated from the oxidation onset (E_{onset}) or $E_{1/2}$ and the onset absorption wavelength of the UV–vis spectra, and the results are listed in Table 3. The high-lying HOMO energy level and reversible electrochemical oxidation of these polymers suggest that they have potential for use as hole injection and transport materials in EL devices.

3.3.4. Spectroelectrochemical and electrochromic properties

Spectroelectrochemical experiments were conducted to elucidate the optical characteristics of the electrochromic films. The electrode preparations and solution conditions were identical to those used in cyclic voltammetry. The results of the **5c** film are presented in Fig. 8 as a series of UV–vis absorbance curves correlated to electrode potentials. In its neutral state, the film exhibited strong absorption at wavelength around 306 nm, characteristic for the TPA moiety, but it was almost transparent in the visible region. When the applied voltage was stepped from 0 to 1.05 V, the intensity of the absorption peak around 306 nm

Table 2
Thermal properties of poly(amide–imide)s[a].

Polymer code	T_g[b] (°C)	T_s[c] (°C)	T_d at 10 wt.% loss[d] (°C)		Char yield[e] (%)
			In N_2	In air	
5a	280	–[f]	504	473	66
5b	281	276	555	543	68
5c	280	279	578	558	71
5d	269	259	555	544	72
5e	313	300	563	555	72
5f	294	276	528	524	71
5g	280	270	529	526	70
5′a	309	–[f]	530	516	69
5′b	297	289	584	564	70
5′c	285	280	614	578	71
5′d	272	255	605	556	70
5′e	326	305	598	578	74
5′f	295	282	555	550	71
5′g	295	290	616	593	75

[a] The polymer film samples were heated at 300 °C for 30 min before all the thermal analyses.
[b] The samples were heated from 50 to 400 °C at a scan rate of 20 °C/min followed by rapid cooling to 50 °C at −200 °C /min in nitrogen. The midpoint temperature of baseline shift on the subsequent DSC trace (from 50 to 400 °C at heating rate 20 °C/min) was defined as T_g.
[c] Softening temperature measured by TMA with a constant applied load of 10 mN at a heating rate of 10 °C/min.
[d] Decomposition temperature at which a 10% weight-loss was recorded by TGA at a heating rate of 20 °C/min and a gas flow rate of 20 cm^3/min.
[e] Residual weight percentages at 800 °C under nitrogen flow.
[f] No available specimens for the TMA testing.

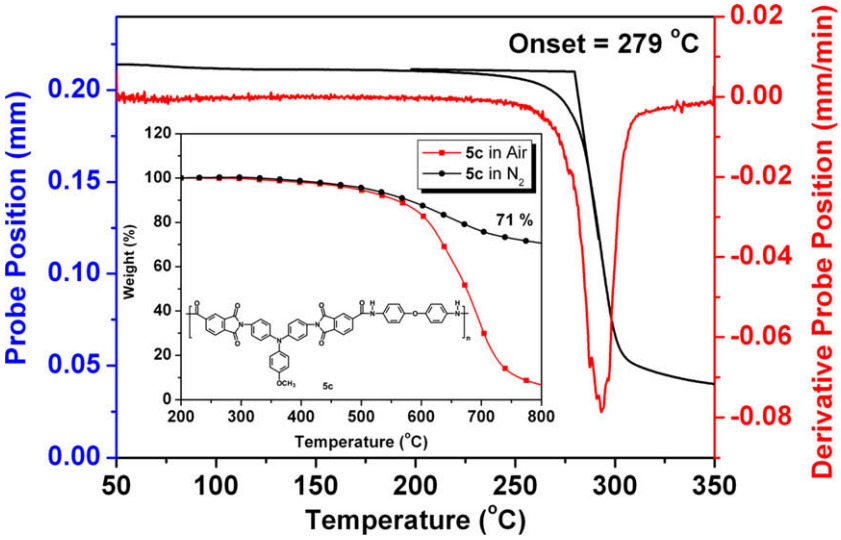

Fig. 5. TMA and TGA curves of PAI **5c** with a heating rate of 10 and 20 °C/min, respectively.

decreased gradually, and new peaks at 374 and 754 nm gradually increased in intensity. We attribute these spectral changes to the formation of a stable cation radical of the TPA moiety. From the inset shown in Fig. 8, it can be seen that the film of PAI **5c** switches from a transmissive neutral state (nearly colorless) to a highly absorbing oxidized state (blue).

For optical switching studies, the polymer film of **5c** was cast on ITO-coated glass slides in the same manner as described above, and the film was potential stepped between its neutral (0.0 V) and oxidized (+1.05 V) state. While the potential was switched, the absorbance at 374 nm and 754 nm was monitored as a function of the time with UV–vis-NIR spectroscopy. The switching time was calculated at 90% of the full switch because it is difficult to perceive any further color change with naked eye beyond this point. The polymer switched rapidly between the highly transmissive neutral state and the colored oxidized state. As depicted in Fig. 9, thin film from PAI **5c** required 6.8 s at 1.05 V for switching absorbance at 754 nm and 1.9 s for bleaching, reflecting the different reaction rates between the neutral and oxidized forms of the film of **5c**. The contrast was measured as the %*T* difference between the neutral and oxidized forms of PAI **5c** and was found to be about 68% at 754 nm. As shown in Fig. 10, the switching stability of the polymer was reasonable

Table 3
Optical and electrochemical properties of PAIs.

Polymer code	In solution		As film		Oxidation potential (V)[b]			E_g[c] (eV)	HOMO[d] (eV)		LUMO[e] (eV)	
	Abs	PL	Abs	Abs	First		Second					
	λ_{max} (nm)[a]	λ_{max} (nm)[a]	λ_{max} (nm)	λ_{onset} (nm)	$E_{1/2}$	E_{onset}	$E_{1/2}$		$E_{1/2}$	E_{onset}	$E_{1/2}$	E_{onset}
5a	292	364	–	–	– (–)	– (–)	– (–)	–	–	–	–	–
5b	302	364	314	453	0.93 (1.07)[f]	0.80 (1.00)	– (–)	2.74	5.29	5.16	2.55	2.42
5c	290	363	313	471	0.91 (1.06)	0.78 (0.99)	– (–)	2.63	5.27	5.14	2.64	2.51
5d	301	366	314	459	0.92 (1.07)	0.79 (1.00)	– (–)	2.70	5.28	5.15	2.58	2.45
5e	310	365	311	459	0.91 (1.05)	0.77 (0.96)	– (–)	2.70	5.27	5.13	2.57	2.43
5f	304	363	312	492	0.82 (0.87)	0.66 (0.70)	0.94 (0.98)	2.56	5.18	5.02	2.62	2.46
5g	306	364	318	485	0.74 (0.86)	0.60 (0.70)	0.93 (1.04)	2.52	5.10	4.96	2.58	2.44

[a] The polymer concentration was 1×10^{-5} mol/L in NMP.
[b] Oxidation half-wave potentials from cyclic voltammograms.
[c] Energy gap = 1240/Abs λ_{onset} of the polymer film.
[d] The HOMO energy levels were calculated from $E_{1/2}$ and were referenced to ferrocene (4.8 eV).
[e] LUMO = HOMO − E_g.
[f] Values in parentheses are data of the analogous **5′** series PAIs.

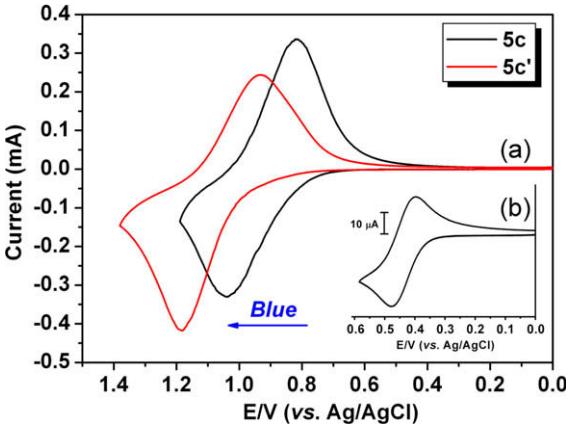

Fig. 6. (a) Cyclic voltammograms of PAI **5c** and **5′c** film on an ITO-coated glass substrate in CH_3CN containing 0.1 M TBAP at scan rate of 50 mV/s. (b) CV curve of ferrocene as a reference.

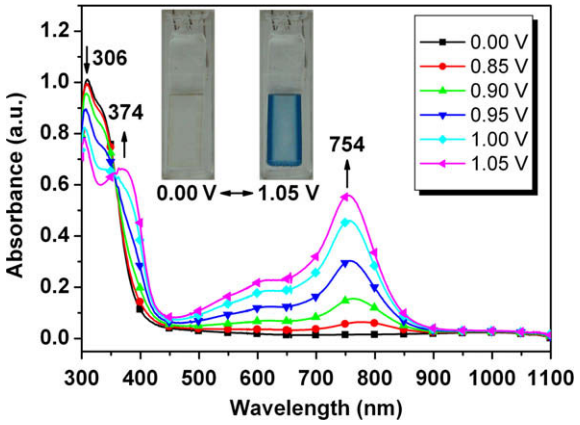

Fig. 8. Spectra and color changes of the cast film of PAI **5c** on ITO-glass in 0.1 M TBAP/CH_3CN solution at various electrode potentials (vs. Ag/AgCl).

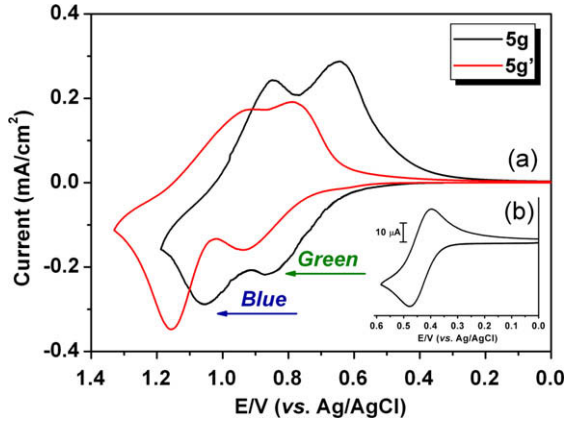

Fig. 7. (a) Cyclic voltammograms of PAIs **5g** and **5′g** film on an ITO-coated glass substrate in CH_3CN containing 0.1 M TBAP at scan rate of 50 mV/s. (b) CV curve of ferrocene as a reference.

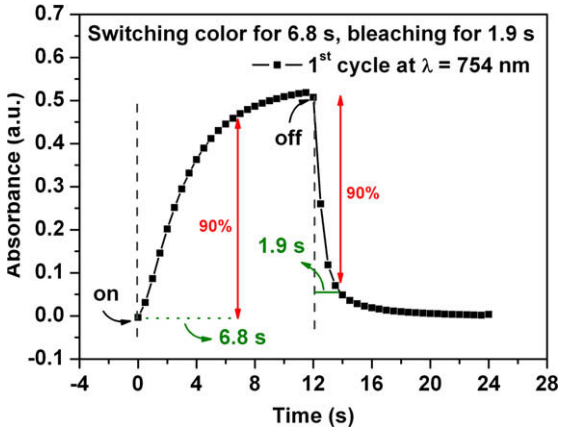

Fig. 9. Dynamic change of the absorbance upon switching the potential between 0.0 and 1.05 V (vs. Ag/AgCl) with a pulse width of 12 s applied to the cast film of polymer **5c** on the ITO-coated glass slide in CH_3CN containing 0.1 M TBAP.

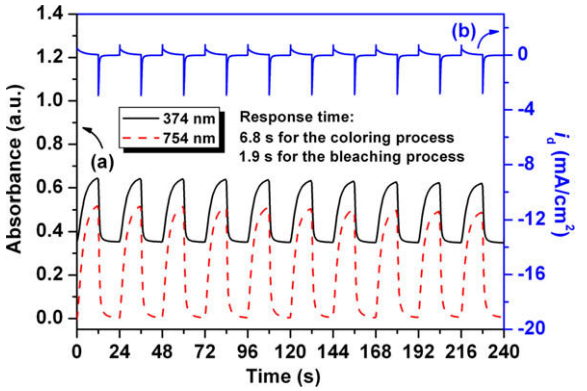

Fig. 10. (a) Optical response (at 374 and 754 nm) and (b) electrical current response as a function of time for the cast film of PAI **5c** on the ITO-coated glass slide (active area ~1 cm^2) (in CH_3CN with 0.1 M TBAP as the supporting electrolyte) by applying a potential step between 0 and 1.05 V, with a cycle time of 24 s. The response time was measured at 754 nm.

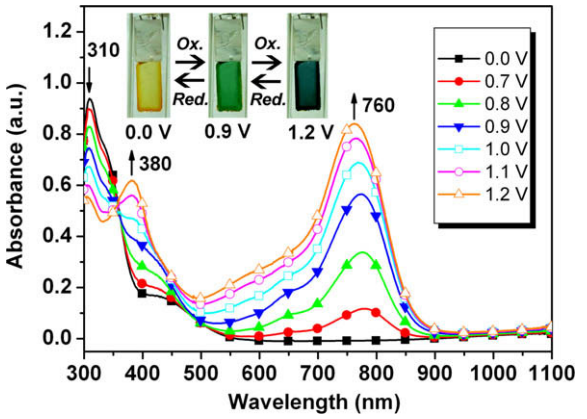

Fig. 11. Spectra and color changes of the cast film of PAI **5g** on ITO-coated glass slide in 0.1 M TBAP/CH_3CN solution at various electrode potentials (vs. Ag/AgCl). (For interpretation of the references to color in this figure legend, the reader is referred to the web version of this article.)

because the optical and current responses were always uniformed in the first 30 switching cycles. Even after hundreds of switching cycles, PAI **5c** did not completely lose its redox and electrochromic activity.

The UV–vis spectral changes at various electrode potentials for the cast film of PAI **5g** are presented in Fig. 11. In the neutral state, this PAI revealed an absorption tail in the region of 400–600 nm in addition to the strong π–π^* transition bands at 310 nm. Therefore, their films exhibited a pale yellow color, not completely colorless, in the neutral state. The absorption tail may be accounted for a stronger interchain charge-transfer interaction between the arylamino donor (in the amide segment) and the trimellitimido acceptor. This PAI presented the multi-electrochromic behavior, because it had two TPA moieties of different electronic nature. PAI **5g** switched from a transmissive, pale yellow neutral state to a green semi-oxidized state and a deep blue fully oxidized state. When the applied voltage was gradually increased from 0 to 0.9 V, the intensity of the absorption peak at 310 nm decreased gradually, and a new peak at 760 nm gradually increased in intensity. We attribute this spectral change to the formation of a stable monocation radical from the TPA moiety in the amide segment. When the potential was adjusted to a more positive value of 1.2 V, the low energy absorption band slightly blue-shifted and an additional new peak centered at about 380 nm appeared. This spectral change indicated the occurrence of the second oxidation from the amino center in the imide segment of PAI **5g**.

4. Conclusions

The diimide-diacid **3** was used as a new building block of poly(amide–imide)s with electrochemically active and stable 4-methoxytriphenylamine unit in the main chain. Because of the presence of the methoxy-substituted TPA unit, all the polymers were amorphous, had good solubility in many polar aprotic solvents, and exhibited excellent film-forming ability. In addition to high T_g values and good thermal stability, all the PAIs were electroactive and electrochromic. The PAIs containing the TPA unit in both imide and amide segments exhibited multicolor electrochromic behavior, with coloration change from neutral pale yellow state to green semi-oxidized state and then to deep blue fully oxidized state. Thus, this new PAI family could be good candidates as anodically electrochromic or hole-transporting materials due to their proper oxidation potentials, good electrochemical stability, and thin film formability.

Acknowledgement

We thank the National Science Council of Taiwan (ROC) for financial support of this work.

References

[1] Monk PMS, Mortimer RJ, Rosseinsky DR. Electrochromism and electrochromic devices. Cambridge: Cambridge University Press; 2007.
[2] Bange K, Gambke T. Electrochromic materials for optical switching devices. Adv Mater 1990;2:10–6.
[3] Rauh RD. Electrochromic windows: an overview. Electrochim Acta 1999;44:3165–76.
[4] Rosseinsky DR, Mortimer RJ. Electrochromic systems and the prospects for devices. Adv Mater 2001;13:783–93.
[5] Heuer HW, Wehrmann R, Kirchmeyer S. Electrochromic window based on conducting poly(3,4-ethylenedioxythiophene)-poly(styrene sulfonate). Adv Funct Mater 2002;12:89–94.
[6] Mortimer RJ, Dyer AL, Reynolds JR. Electrochromic organic and polymeric materials for display applications. Displays 2006;27:2–18.
[7] Anderson P, Forchheimer R, Tehrani P, Berggren M. Printable all-organic electrochromic active-matrix displays. Adv Funct Mater 2007;17:3074–82.
[8] Niklasson GA, Granqvist CG. Electrochromics for smart windows: thin films of tungsten oxide and nickel oxide, and devices based on these. J Mater Chem 2007;17:127–56.
[9] Beaupre S, Breton AC, Dumas J, Leclerc M. Multicolored electrochromic cells based on poly(2,7-carbazole) derivatives for adaptive camouflage. Chem Mater 2009;21:1504–13.
[10] Baetens R, Jelle BP, Gustavsen A. Properties, requirements and possibilities of smart windows for dynamic daylight and solar energy control in buildings: a state-of-the-art review. Sol Energy Mater Sol Cells 2010;94:87–105.

[11] Mortimer RJ. Electrochromic materials. Chem Soc Rev 1997;26:147–56.
[12] Lee S-H, Deshpande R, Parilla PA, Jones KM, To B, Mahan H, et al. Crystalline WO_3 nanoparticles for highly improved electrochromic applications. Adv Mater 2006;18:763–6.
[13] Han FS, Higuchi M, Kurth DG. Metallosupramolecular polyelectrolytes self-assembled from various pyridine ring-substituted bisterpyridines and metal ions: photophysical, electrochemical, and electrochromic properties. J Am Chem Soc 2008;130:2073–81.
[14] Maier A, Rabindranath R, Tieke B. Fast-switching electrochromic films of zinc polyiminofluorene-terpyridine prepared upon coordinative supramolecular assembly. Adv Mater 2009;21:959–63.
[15] Patra A, Bendikov M. Polyselenophenes. J Mater Chem 2010;20:422–33.
[16] Groenendaal L, Zotti G, Aubert P-H, Waybright SM, Reynolds JR. Electrochemistry of poly(3,4-alkylenedioxythiophene) derivatives. Adv Mater 2003;15:855–79.
[17] Walczak RM, Reynolds JR. Poly(3,4-alkylenedioxypyrroles): the PXDOPs as versatile yet underutilized electroactive and conducting polymers. Adv Mater 2006;18:1121–31.
[18] Beaujuge PM, Reynolds JR. Color control in π-conjugated organic polymers for use in electrochromic devices. Chem Rev 2010;110:268–320.
[19] Sonmez G, Sonmez HB, Shen CKF, Jost RW, Rubin Y, Wudl F. A processable green polymeric electrochromic. Macromolecules 2005;38:669–75.
[20] Sonmez G. Polymeric electrochromics. Chem Commun 2005:5251–9.
[21] Wu C-G, Lu M-I, Chang S-J, Wei C-S. A solution-processable high-coloration-efficiency low-switching-voltage electrochromic polymer based on polycyclopentadithiophene. Adv Funct Mater 2007;17:1063–70.
[22] Balan A, Gunbas GE, Durmus A, Toppare L. Donor-acceptor polymer with benzotriazole moiety: enhancing the electrochromic properties of the "donor unit". Chem Mater 2008;20:7510–3.
[23] Celebi S, Balan A, Epik B, Baran D, Toppare L. Donor acceptor type neutral state green polymer bearing pyrrole as the donor unit. Org Electron 2009;10:631–6.
[24] Cihaner A, Algi F. A novel neutral state green polymeric. electrochromic with superior n- and p-doping processes: closer to red-blue-green (RGB) display realization. Adv Funct Mater 2008;18:3583–9.
[25] Pamuk M, Tirkes S, Cihaner A, Algi F. A new low-voltage-driven polymeric electrochromic. Polymer 2010;51:62–8.
[26] Thelakkat M. Star-shaped, dendrimeric and polymeric triarylamines as photoconductors and hole transport materials for electro-optical applications. Macromol Mater Eng 2002;287:442–61.
[27] Shirota Y, Kageyama H. Charge carrier transporting molecular materials and their applications in devices. Chem Rev 2007;107:953–1010.
[28] Beaupre S, Dumas J, Leclerc M. Toward the development of new textile/plastic electrochromic cells using triphenylamine-based copolymers. Chem Mater 2006;18:4011–8.
[29] Natera J, Otero L, Sereno L, Fungo F, Wang N-S, Tsai Y-M, et al. A novel electrochromic polymer synthesized through electropolymerization of a new donor-acceptor bipolar system. Macromolecules 2007;40:4456–63.
[30] Cheng S-H, Hsiao S-H, Su T-H, Liou G-S. Novel aromatic poly (amine-imide)s bearing pendent triphenylamine group: synthesis, thermal, photophysical, electrochemical, and electrochromic characteristics. Macromolecules 2005;38:307–16.
[31] Hsiao S-H, Chang Y-M, Chen H-W, Liou G-S. Novel aromatic polyamides and polyimides functionalized with 4-*tert*-butyltriphenylamine groups. J Polym Sci A: Polym Chem 2006;44:4579–92.
[32] Chang C-W, Liou G-S, Hsiao S-H. Highly stable anodic green electrochromic aromatic polyamides: synthesis and electrochromic properties. J Mater Chem 2007;17:1007–15.
[33] Hsiao S-H, Liou G-S, Kung Y-C, Yen H-J. High contrast ratio and rapid switching electrochromic polymeric films based on 4-(dimethylamino)triphenylamine-functionalized aromatic polyamides. Macromolecules 2008;41:2800–8.
[34] Kung Y-C, Liou G-S, Hsiao S-H. Synthesis and characterization of novel electroactive polyamides and polyimides with bulky 4-(1-adamantoxy)triphenylamine moieties. J Polym Sci A: Polym Chem 2009;47:1740–55.
[35] Hsiao S-H, Liou G-S, Kung Y-C, Pan H-Y, Kuo C-H. Electroactive aromatic polyamides and polyimides with adamantylphenoxy-substituted triphenylamine units. Eur Polym J 2009;45:2234–48.
[36] Yen H-J, Liou G-S. Solution-processable novel near-infrared electrochromic aromatic polyamides based on electroactive tetraphenyl-*p*-phenylenediamine moieties. Chem Mater 2009;21:4062–70.
[37] Ghosh MM, Mittal KL, editors. Polyimides: fundamentals and applications. New York: Marcel Dekker; 1996.
[38] Imai Y. Synthesis of polyamideimides. In: Ghosh MM, Mittal KL, editors. Polyimide: fundamentals and applications. New York: Marcel Dekker; 1996. p. 49–70.
[39] Behniafar H, Banihashemi A. Synthesis and characterization of new soluble and thermally stable aromatic poly(amide-imide)s based on *N*-[3,5-bis(*N*-trimellitoyl)phenyl]phthalimide. Eur Polym J 2004;40:1409–15.
[40] Sarkar A, Honkhambe PN, Avadhani CV, Wadgaonkar PP. Synthesis and characterization of poly(amideimide)s containing pendent flexible alkoxy chains. Eur Polym J 2007;43:3646–54.
[41] Yamazaki N, Matsumoto M, Higashi F. Studies on reactions of the *N*-phosphonium salts of pyridines. XIV. Wholly aromatic polyamides by the direct polycondensation reaction by using phosphites in the presence of metal salts. J Polym Sci Polym Chem Ed 1975;13:1373–80.
[42] Yang C-P, Hsiao S-H. Preparation of poly(amide-imide)s by means of triphenyl phosphite, 1. Aliphatic-aromatic poly(amide-imide)s based on trimellitimide. Makromol Chem 1989;190:2119–31.
[43] Hsiao S-H, Yang C-P. Preparation of polyamide-imides via the phosphorylation reaction. II. Synthesis of wholly aromatic polyamide-imides from *N*-[*p*-(or *m*)carboxyphenyl]trimellitimides and various aromatic diamines. J Polym Sci A: Polym Chem 1990;28:1149–59.
[44] Chern Y-T, Huang C-M, Huang S-C. Synthesis and characterization of new poly(amide-imide)s containing 4,9-diamantane moieties in the main chain. Polymer 1998;39:2929–34.
[45] Liaw D-J, Hsu P-N, Chen W-H, Liaw B-Y. Novel organosoluble poly(amide-imide)s derived from kink diamine bis[4-(4-trimellitimidophenoxy)phenyl]-diphenylmethane. Synthesis and characterization. Macromol Chem Phys 2001;202:1483–7.
[46] Lee C, Iyer NP, Min K, Pak H, Han H. Synthesis and characterization of novel poly(amide-imide)s containing 1,3-diamino mesitylene moieties. J Polym Sci A: Polym Chem 2004;42:137–43.
[47] Hsiao S-H, Yang C-P, Chen C-W, Liou G-S. Synthesis and properties of novel aromatic poly(amide-imide)s containing pendent diphenylamino groups. Eur Polym J 2005;41:511–7.
[48] Behniafar H, Haghigha S. Preparation and properties of aromatic poly(amide-imide)s derived from *N*-[3,5-bis(3,4-dicarboxybenzamido)phenyl]phthalimide dianhydride. Eur Polym J 2006;42:3236–47.
[49] Oishi Y, Takado H, Yoneyama M, Kakimoto M, Imai Y. Preparation and properties of new aromatic polyamides from 4,4-diaminotriphenylamine and aromatic dicarboxylic acids. J Polym Sci A: Polym Chem 1990;28:1763–9.
[50] Demas JN, Crosby GA. Measurement of photoluminescence quantum yields. Review. J Phys Chem 1971;75:991–1024.